

Quantized Hall conductance and its sign reversal in field-induced spin-density waves

K. Machida

Department of Physics, Okayama University, Okayama 700, Japan

Y. Hasegawa

Faculty of Science, Himeji Institute of Technology, Akou-gun, Hyogo 678-12, Japan

M. Kohmoto

Institute of Solid State Physics, University of Tokyo, Roppongi, Minato-ku, Tokyo 106, Japan

V. M. Yakovenko

Department of Physics, University of Maryland, College Park, Maryland 20742-4111

Y. Hori and K. Kishigi

Department of Physics, Okayama University, Okayama 700, Japan

(Received 22 November 1993)

The sign-reversal phenomenon of the quantized Hall conductance as a function of an external magnetic field (H) observed in $(\text{TMTSF})_2X$ is investigated theoretically. After giving a general Hall-conductance formula written in terms of order parameters of the field-induced spin-density wave (FISDW), we have done extensive mean-field calculations for a simplified standard model. It is shown that the many competing order parameters Δ_n ($n=0, \pm 1, \pm 2, \dots$) which coexist in a FISDW state can make the sign of the Hall constant change particularly near the subphase boundary of the FISDW and that numbering of the integer subphases ($N=0, 1, 2, \dots$ stabilized in this order from high fields) does not necessarily coincide with the Hall number L defined by $L = \sigma_{xy}/(e^2/h)$. We have found that the jumps of the Hall constant are accompanied by the spin-density wave gap closing when a FISDW is continuously evolving as H varies. In order for the sign reversal to occur a FISDW must contain many order parameters Δ_n with n being both signs.

I. INTRODUCTION

Much attention¹ has been focused on the field-induced spin-density wave (FISDW) transitions in quasi-two-dimensional organic conductors $(\text{TMTSF})_2X$ (where TMTSF is tetramethyltetraselenafulvalene and $X = \text{ClO}_4$, PF_6 , and ReO_4). This phenomenon has been investigated theoretically² and understood as “one-dimensionalization” of the two-dimensional electron motion under perpendicular magnetic fields (H), thereby leading to the Peierls instability for the electron-hole channel toward spin-density-wave formation. The calculations based on the so-called standard model,³⁻⁷ namely, the anisotropic two-dimensional Hubbard model under perpendicular field, account for the observed phase diagram of H vs T (temperature) shown in the top panel of Fig. 1,⁸ where the integer subphases characterized by integers $N=0, 1, 2, \dots$, from high field are separated by a series of first-order transitions signaled by the peaks in the diagonal resistance $\rho_{xx}(H)$ as depicted in Fig. 1(b).

So far the standard theory is quite successful in giving the overall phase boundary between the normal and the FISDW state. However, two mysteries remain unexplained. (1) The cascade phenomenon of the successive SDW transitions⁹ inside the integer subphases at lower temperatures in ClO_4 , giving rise to infinitely many FISDW states in the H vs T plane, and (2) the so-called

Rebault anomaly,¹⁰ namely, the sign reversals of the quantized Hall conductivity $\sigma_{xy}(H) = L \frac{e^2}{h}$ (L can take both signs) as a function of H . This sign-reversal phenomenon was first observed with $X = \text{ClO}_4$,^{10,11} and now with PF_6 (Refs. 8, 12, and 13) and ReO_4 (Ref. 14) as well, and is regarded as a universal phenomenon associated with the FISDW.

These two mysteries cannot be accounted for in terms of the standard theory in its naive form³⁻⁵ where a subphase N is uniquely characterized by a single SDW order parameter Δ_N with the wave number $Q_x = 2k_F + N\delta$ [k_F is the Fermi wave number and $\delta^{-1} (= \hbar c / ebH)$ the magnetic length, where b is the lattice spacing of the y axis]. Thus there exist no more countable subphases other than $N=0, 1, 2, 3$, etc., which are unable to account for the infinitely many FISDW subphases observed, corresponding to the cascade phenomenon mentioned above. According to Poilblanc *et al.*,¹⁵ who prove the quantization of the Hall constant in the present bulk system by utilizing the Štředa formula,¹⁶ a subphase characterized by Δ_L uniquely yields $\sigma_{xy} = L e^2/h$ with the quantized Hall number L ($L=0, 1, 2, \dots$). If this is true, the Hall constant is just a monotonic function of H and exhibits no sign reversal unless the arrangement of the subphases includes both positive and negative integer subphases in some irregular way.

In Fig. 1(c) we display the Hall conductivity $\sigma_{xy}(H)$,

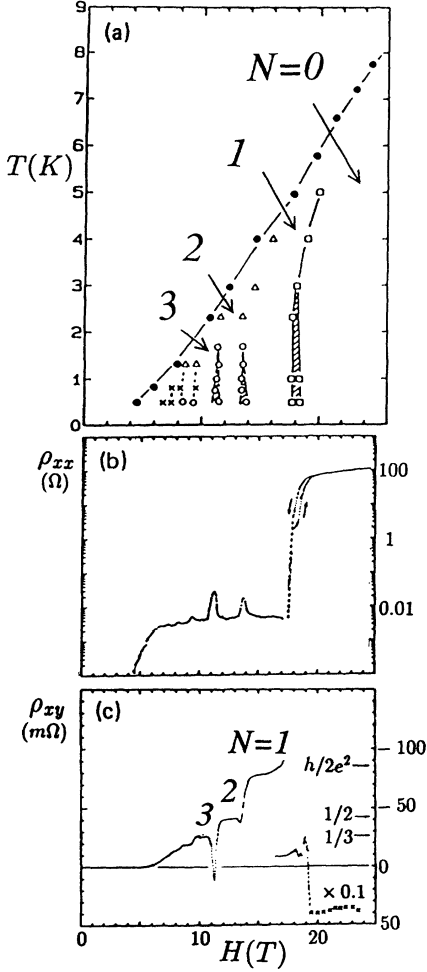


FIG. 1. Experimental results on $(\text{TMTSF})_2\text{PF}_6$ obtained by Cooper *et al.* (Ref. 8). (a) H vs T phase diagram. (b) Peaks in the diagonal resistivity $\rho_{xx}(H)$ at $T=0.5$ K. (c) Hall resistance $\rho_{xy}(H)$ showing the quantized Hall plateaus approximately corresponding to each integer subphase numbering. A negative-Hall-constant region exists between the $N=2$ and $N=3$ subphases which are expected to give the Hall numbers $L=2$ and $L=3$ respectively in the naive standard theory.

showing the quantized Hall plateaus approximately corresponding to each integer subphase. However, between the $N=2$ and $N=3$ subphases, which are expected to give rise to the Hall numbers $L=2$ and $L=3$, respectively, within the framework of the naive standard theory,^{3–5} there exists a negative-Hall-constant region. It is unlikely that the integer subphase with $N < 0$ ($N=-2$ or -3) intrudes between $N=2$ and $N=3$, because the subphases in $X=\text{PF}_6$ under pressure are known to be arranged regularly $N=0, 1, 2, \dots$ from high fields in accord with the standard theory in all other respects.^{1,8,11} As for $X=\text{ReO}_4$,¹⁴ the negative-Hall-constant region is quite large ($12 < H < 16$ T) followed by the positive-Hall-constant plateaus in high fields. Again it is unlikely that such a large H region is occupied by the subphases with negative integers. In $X=\text{ClO}_4$ the cooling-rate dependences of the phase diagram¹⁷ and Hall measurements^{10,11} reveal an interesting coincidence between these two quantities, namely, the phase produced

around 5.5–6.3 T by slowly cooling samples, which is absent in rapid-cooling experiments, indeed is responsible for the negative Hall constant. This means that the conventionally assigned integer number for a subphase does not necessarily correspond to the Hall number, which is in disagreement with Poilblanc *et al.*¹⁵ All these experimental data point to something important missing in the naive standard theory.^{3–5}

Previously⁷ we have found in connection with the cascade phenomenon that the FISDW phase is in general characterized by a set $\{\Delta_n\}$ (n is a rational number) of many order parameters (MOP's), namely, the coexistence of multiple OP's, while the naive standard theory is assumed to be described by a single order parameter (SOP) as mentioned above. The number of the MOP states is infinite, corresponding to the fact that the combination of many OP's is practically infinite and this is capable of accounting for the infinitely many FISDW subphases in the ground state.

One of the authors¹⁸ set up a formula for the quantized Hall constant of the FISDW phase under a given set of many OP's, based on the argument due to Thouless *et al.*,¹⁹ who demonstrate that the Hall constant is a topological number (Chern number) and quantized in a two-dimensional electron system on a lattice under H , starting with the Kubo formula. Indeed as Hasegawa *et al.*²⁰ have shown explicitly, the energy gaps between the Landau bands in the so-called Hofstadter butterfly diagram²¹ correspond to integers with both signs.

The purposes of this paper²² are to demonstrate (1) that the quantized Hall number L can take both signs even for an integer subphase N which consists of multiple order parameters $\{\Delta_n\}$ ($n=0, \pm 1, \pm 2, \dots$) with Δ_N being the largest and L not necessarily equal to N , and (2) that under varying parameters of the problem, i.e., H , the Hall number $L(H)$ changes in a stepwise manner, including the sign change, even when the order parameters evolve continuously.

II. FORMULATION OF THE PROBLEM

The quasi-one-dimensional organic conductors in this class of materials are described in terms of an anisotropic Hubbard model,

$$\begin{aligned} \mathcal{H} = & -t_a \sum_{(i,j)_x, \sigma} c_{i,\sigma}^\dagger c_{j,\sigma} - t_b \sum_{(i,j)_y, \sigma} c_{i,\sigma}^\dagger c_{j,\sigma} \\ & + U \sum_i c_{i,\uparrow}^\dagger c_{i,\uparrow} c_{i,\downarrow}^\dagger c_{i,\downarrow}, \end{aligned} \quad (2.1)$$

where $c_{i,\sigma}^\dagger$ and $c_{i,\sigma}$ are the creation and annihilation operators of electrons, respectively, t_a and t_b are the hopping matrix elements along the a and b directions, respectively, and the hopping along the c direction is neglected for simplicity. Because of the anisotropy ($t_b/t_a \approx 0.1$), the Fermi surface consists of two warped lines for the quarter-filled case, which is the case of $(\text{TMTSF})_2X$.

First, we consider the noninteracting case, $U=0$. In the presence of an external magnetic field H the original Brillouin zone is reduced and the Hamiltonian is written²⁰

$$\mathcal{H} = \sum_{k_F - \delta/2 \leq k_x < k_F + \delta/2} \sum_{-\pi/b \leq k_y < \pi/b} \sum_{\sigma} c_{\sigma}^{\dagger}(k_x, k_y) \times \begin{bmatrix} \ddots & & & & -t_b e^{-ibk_y} \\ & -2t_a \cos[a(k_x - \delta)] & -t_b e^{ibk_y} & 0 & \\ & -t_b e^{-ibk_y} & -2t_a \cos(ak_x) & -t_b e^{ibk_y} & \\ & 0 & -t_b e^{-ibk_y} & -2t_a \cos[a(k_x + \delta)] & \\ -t_b e^{ibk_y} & & & & \ddots \end{bmatrix} c_{\sigma}(k_x, k_y), \quad (2.2)$$

where a and b are the lattice constants, $\delta = ebH/(\hbar c)$, i.e., $a\delta = 2\pi\phi/\phi_0$, $\phi = abH$ is the flux per unit cell $a \times b$, $\phi_0 = hc/e$ is the flux quantum, and

$$c_{\sigma}^{\dagger} = [\dots, c_{\sigma}^{\dagger}(k_x - \delta, k_y), c_{\sigma}^{\dagger}(k_x, k_y), c_{\sigma}^{\dagger}(k_x + \delta, k_y), \dots]. \quad (2.3)$$

We have neglected the Zeeman effect for simplicity since it does not alter the essential part of the result. The off-diagonal term, $-t_b \exp(\pm ibk_y)$, mixes the wave functions for wave numbers (k_x, k_y) and $(k_x \pm \delta, k_y)$. It is to be noticed that, if $\phi/\phi_0 = q/p$ with integers $q \neq 1$ and p , the width of the Brillouin zone in the k_x direction is actually not δ but δ/q . However, for a small field [$a\delta \approx 10^{-3}$ in the experiments for $(\text{TMTSF})_2\text{X}$] and small t_b/t_a , one can neglect this effect, which splits each Landau band into q subbands.

The Hall conductance from a filled band is calculated by the general formula, starting from the Kubo formula, as¹⁹

$$\begin{aligned} \sigma_{xy} &= 2 \frac{e^2}{h} \frac{1}{2\pi i} \int_{k_F - \delta/2}^{k_F + \delta/2} dk_x \int_{-\pi/b}^{\pi/b} dk_y \left[\left[\frac{\partial}{\partial k_x} \langle \Psi | \right] \left[\frac{\partial}{\partial k_y} | \Psi \rangle \right] - \left[\frac{\partial}{\partial k_y} \langle \Psi | \right] \left[\frac{\partial}{\partial k_x} | \Psi \rangle \right] \right] \\ &= 2 \frac{e^2}{h} \frac{1}{2\pi i} \int_{k_F - \delta/2}^{k_F + \delta/2} dk_x \int_{-\pi/b}^{\pi/b} dk_y \left[\frac{\partial}{\partial k_x} \left[\langle \Psi | \frac{\partial}{\partial k_y} | \Psi \rangle \right] - \frac{\partial}{\partial k_y} \left[\langle \Psi | \frac{\partial}{\partial k_x} | \Psi \rangle \right] \right], \end{aligned} \quad (2.4)$$

where $|\Psi(k_x, k_y)\rangle$ is the wave function at the wave number (k_x, k_y) . This is a topological expression, giving rise to the Chern number. The factor of 2 comes from the summation over the spin index. The second term vanishes because of the periodicity in the k_y direction. The first term is finite when the wave function changes its character when crossing an energy gap. The contribution to σ_{xy} from the lower edge of the r th band from the bottom cancels with that from the upper edge of the $(r-1)$ th band. Therefore, the Hall conductance is obtained as the winding number at the Fermi level E_F and we get²³

$$\begin{aligned} \sigma_{xy} &= 2 \frac{e^2}{h} \frac{1}{2\pi i} \left[\int_{-\pi/b}^{\pi/b} dk_y \left[\left\langle \Psi \left| \frac{\partial}{\partial k_y} \right| \Psi \right\rangle \right]_{k_x = -\kappa} \right. \\ &\quad \left. - \left\langle \Psi \left| \frac{\partial}{\partial k_y} \right| \Psi \right\rangle \right]_{k_x = +\kappa} \right], \end{aligned} \quad (2.5)$$

where $k_x = \pm\kappa$ are the momenta at the opposite sides of the Fermi momentum. It has been shown that, when the chemical potential is in a gap below which r bands are completely filled, the Hall conductance for each spin is given by¹⁹

$$\sigma_{xy} = -\frac{e^2}{h} t_r, \quad (2.6)$$

where t_r is the solution of the Diophantine equation

$$r = ps_r + qt_r, \quad (2.7)$$

with $|t_r| < p/2$ and integers p and q defined above. If $q=1$ and $2k_F/\delta$ is an integer, we get $r=2k_F/\delta$. The solution of the Diophantine equation is $s_r=0, t_r=r$ for the less than half-filled case, $|r| < p/2$. For the more than half-filled case the solution is $s_r=1, t_r=r-p < 0$. This can be understood as follows. The state at k_F mixes with that at $-k_F$ by the $|t_r|$ th perturbation in t_b/t_a and a gap of the order of $t_a(t_b/t_a)^{|t_r|}$ opens at the Fermi energy. Since the wave function changes the phase of $\exp(ibk_y t_r)$ when crossing the energy gap, we get $\sigma_{xy} = t_r e^2/h$. In the above calculation for the less than half-filled case we get the same Hall conductance as that for free electrons in two dimensions, in which t_r Landau levels are completely filled, although each Landau level becomes a band due to the lattice effects. For the more than half-filled case, the sign of the Hall conductance is reversed and the holelike quantized Hall effect takes place. All contributions of electrons below the Fermi energy are correctly calculated from the property of the wave function near the Fermi energy. When $q \neq 1$, the subband structure differs from the case of $q=1$. The resulting Hall number t_r may be different. In the realistic magnetic-field region of $2k_F/\delta \approx 1000$, that is, p is quite large, the energy gaps in the Hofstadter spectrum are too small to observe the quantized Hall effect. However, the situation is drastically changes if a new periodicity is created by a FISDW as we will discuss below.

Now let us consider the effect of the interaction U . Since the Hall conductance is obtained from the properties near the Fermi level as discussed above, we can

linearize the dispersion along the k_x direction around E_F and we get

$$\epsilon(\mathbf{k}) = v_F(|k_x| - k_F) + \epsilon_\perp(k_y), \quad (2.8)$$

where $v_F = |2t_a a \sin(ak_F)|$, and

$$\epsilon_\perp(k_y) = -2t_b \cos(bk_y) - 2t'_b \cos(2bk_y), \quad (2.9)$$

in which t'_b is introduced to break the nesting of the Fermi surface and can be given as a perturbation³ in t_b/t_a by

$$t'_b = -t_b^2 \cos(ak_F) / [4t_a \sin^2(ak_F)].$$

This is the so-called standard model widely adopted to describe Bechgaard salts. The Hamiltonian in the presence of a magnetic field H is now written^{4,18} as

$$\mathcal{H} = \sum_{\sigma} \int_{-\pi/b}^{\pi/b} \frac{dQ_y}{2\pi/b} \int_{-\pi/b}^{\pi/b} \frac{dk_y}{2\pi/b} \int_{-\infty}^{\infty} dx \psi^{\dagger} \begin{pmatrix} -i\hbar v_F \partial_x + \epsilon_{\perp} \left[k_y - \frac{\delta x}{b} \right] & \Delta(x, Q_y) \\ \Delta^*(x, Q_y) & i\hbar v_F \partial_x + \epsilon_{\perp} \left[k_y - \frac{\delta x}{b} + Q_y \right] \end{pmatrix} \psi, \quad (2.10)$$

where

$$\psi(x, k_y, Q_y) \equiv \begin{pmatrix} e^{-ik_F x} \psi_{+, \sigma}(x, k_y) \\ e^{ik_F x} \psi_{-, \sigma}(x, k_y + Q_y) \end{pmatrix}, \quad (2.11)$$

with $\psi_{+, \sigma}(x, k_y)$ ($\psi_{-, \sigma}(x, k_y)$) being the field operator for right-going (left-going) electrons. The ϵ_{\perp} term in the diagonal elements becomes an element connecting k_x and $k_x \pm \delta$ when a Fourier transformation with respect to x is performed. In Eq. (2.10) the off-diagonal element $\Delta(x, Q_y)$ is derived from the on-site Hubbard interaction U by a mean-field approximation. The interaction term is written

$$\begin{aligned} \mathcal{H}' &= U \int_{-\infty}^{\infty} dx \sum_{y_i} \psi_{\uparrow}^{\dagger}(x, y_i) \psi_{\uparrow}(x, y_i) \psi_{\downarrow}^{\dagger}(x, y_i) \psi_{\downarrow}(x, y_i) \\ &= -U \sum_{\sigma} \int_{-\infty}^{\infty} dx \int_{-\pi/b}^{\pi/b} \frac{dk_y}{2\pi/b} \int_{-\pi/b}^{\pi/b} \frac{dk'_y}{2\pi/b} \int_{-\pi/b}^{\pi/b} \frac{dQ_y}{2\pi/b} \psi_{+, \sigma}^{\dagger}(x, k_y) \psi_{-, \sigma}(x, k_y + Q_y) \\ &\quad \times \psi_{-, \sigma}^{\dagger}(x, k'_y + Q_y) \psi_{+, \sigma}(x, k'_y). \end{aligned} \quad (2.12)$$

The order parameter is defined by the mean field of the spin-density wave as

$$\begin{aligned} \Delta(x, Q_y) &\equiv -U \int_{-\pi/b}^{\pi/b} \frac{dk'_y}{2\pi/b} \langle \psi_{-, \sigma}^{\dagger}(x, k'_y + Q_y) \\ &\quad \times \psi_{+, \sigma}(x, k'_y) \rangle. \end{aligned} \quad (2.13)$$

Note that the order parameter depends on x and Q_y . We assume $\Delta(x, Q_y) = \Delta(x) \delta(Q_y - Q_y^0)$, i.e., the Q_y component of the spin-density wave is fixed as Q_y^0 .

There are two types of couplings which connect the states. One is the coupling due to the magnetic field ϕ which connects states at k_x and $k_x \pm \delta$ and the other is the coupling due to the SDW. In order to connect the states at k_F and $-k_F$ the order parameter must be in the form

$$\Delta(x) = \sum_n \Delta_n \exp(in\delta x). \quad (2.14)$$

Then in terms of Δ_n these two states are coupled by $\Delta_n t_b^n \exp(-inbk_y)$ ($n=0, \pm 1, \pm 2, \dots$) (see Fig. 2).

The Hall conductance is evaluated from Eq. (2.5) as $\sigma_{xy} = -2Ne^2/h$ for a single-order-parameter state with Δ_N . The factor of 2 in this expression is not due to the spin degeneracy but should be understood as follows. If we start from the spin up and go around the Brillouin

zone in the k_x direction, we return at the end to the same state but with the spin down. In order to restore the initial spin it is necessary to go around the Brillouin zone another time, and thus the total winding number is doubled.

When the order parameter $\Delta(x) = \Delta_N \exp(iN\delta x)$ exists,

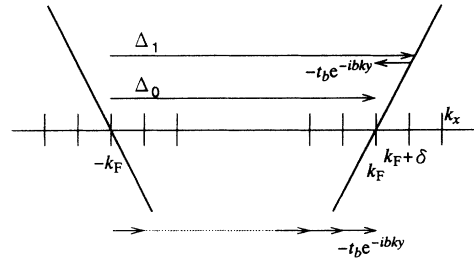


FIG. 2. Schematic diagram of the coupling scheme of the states at $k_x = k_F$ and $k_x = -k_F$. The wave function at $k_x = k_F$ is coupled with that at $k_x = -k_F$ in the t_b th perturbation in (t_b/t_a) (short right-going arrows), resulting in a factor of $\exp(it_b k_y)$. In the presence of the order parameter of the FISDW, coupling is also possible by using the SDW order parameter (long right-going arrow, Δ_0) with a k_y -independent factor or by a combination of the SDW order parameter and the t_b term such as $\Delta_n t_b \exp(-int_b k_y)$ ($n = \pm 1, \pm 2, \dots$, etc.) where Δ_0 directly connects the states at $k_x = \pm k_F$.

the periodicity in the k_x direction is $2\pi/(|N|\delta)$. The flux piercing through a supercell of $2\pi/(|N|\delta) \times b$ is

$$\frac{2\pi}{|N|\delta} bH = \frac{1}{|N|} \phi_0. \quad (2.15)$$

Therefore, the physics at an extremely high magnetic field, such as the problems studied by Hofstadter,²¹ can

be realized by a moderate magnetic field due to the supercell enlarged by the formation of the SDW. The size of the supercell is adjusted so that the flux per supercell is a constant rational number, resulting in a plateau of the Hall conductance since the chemical potential is pinned in the SDW gap.

In order to see this more explicitly, we transform the wave function as^{4,18}

$$\begin{pmatrix} e^{-ik_F x} \psi_{+, \sigma}(x, k_y) \\ e^{ik_F x} \psi_{-, \sigma}(x, k_y + Q_y) \end{pmatrix} = \begin{pmatrix} \psi'_{+, \sigma}(x, k_y) \exp \left[-\frac{ib}{\hbar v_F \delta} \int_0^{\delta x/b} d\xi \epsilon_1(k_y - \xi) \right] \\ \psi'_{-, \sigma}(x, k_y + Q_y) \exp \left[\frac{ib}{\hbar v_F \delta} \int_0^{\delta x/b} d\xi \epsilon_1(k_y + Q_y - \xi) \right] \end{pmatrix}. \quad (2.16)$$

The Hamiltonian is written in terms of $\psi'_{+, \sigma}(x, k_y)$ and $\psi'_{-, \sigma}(x, k_y + Q_y)$ as

$$\mathcal{H} = \sum_{\sigma} \int_{-\pi/b}^{\pi/b} \frac{dk_y}{2\pi/b} \int_{-\infty}^{\infty} dx [\psi'^{\dagger}_{+, \sigma}(x, k_y), \psi'^{\dagger}_{-, \sigma}(x, k_y + Q_y^0)] \begin{pmatrix} -i\hbar v_F \partial_x & \bar{\Delta}(x, k_y) \\ \bar{\Delta}^*(x, k_y) & i\hbar v_F \partial_x \end{pmatrix} \begin{pmatrix} \psi'_{+, \sigma}(x, k_y) \\ \psi'_{-, \sigma}(x, k_y + Q_y^0) \end{pmatrix}, \quad (2.17)$$

where

$$\begin{aligned} \bar{\Delta}(x, k_y) &= \Delta(x) \exp \left\{ \frac{ib}{\hbar v_F \delta} \int_0^{\delta x/b} d\xi [\epsilon_1(k_y - \xi) \right. \\ &\quad \left. + \epsilon_1(k_y - Q_y^0 - \xi)] \right\} \\ &= \Delta(x) e^{-i\Phi(0)} \sum_{n=-\infty}^{\infty} I_n(\alpha, \beta) e^{in\delta(x-x_0)}, \end{aligned} \quad (2.18)$$

where $q_y = Q_y - \pi/b$, $x_0 = b(k_y - q_y/2)/\delta$
 $= (k_y - q_y/2)\hbar c/eH$,

$$\Phi(x) = -\alpha \sin[2\delta(x - x_0)] + \beta \cos[\delta(x - x_0)], \quad (2.19)$$

$$\alpha = 2t'_b \cos(bq_y)/\hbar v_F \delta = \cos(bq_y)/\tilde{H}, \quad (2.20)$$

$$\beta = 4t_b \sin(bq_y/2)/\hbar v_F \delta = \eta \sin(bq_y/2)/\tilde{H}, \quad (2.21)$$

with $\tilde{H} = ev_F bH/2ct'_b$, $\eta = 2t_b/t'_b$, and

$$I_n(\alpha, \beta) = i^n \sum_{l=-\infty}^{\infty} J_l(\alpha) J_{n-2l}(\beta). \quad (2.22)$$

The k_y dependence comes through x_0 .

We perform a Fourier transformation for $\psi'_{\pm, \sigma}$ with respect to x as

$$\psi'_{\pm, \sigma}(x, k_y) = \int_{-\pi/a}^{\pi/a} \frac{dk_x}{2\pi/a} \tilde{\psi}'_{\pm, \sigma}(k_x, k_y) e^{ik_x x}, \quad (2.23)$$

where we have restored the extended Brillouin zone in the k_x direction. The momentum k_x is measured from k_F for $\tilde{\psi}'_+$ and from $-k_F$ for $\tilde{\psi}'_-$. Finally, we get

$$\begin{aligned} \mathcal{H} &= \sum_{\sigma} \int_{-\pi/b}^{\pi/b} \frac{dk_y}{2\pi/b} \int_{-\pi/a}^{\pi/a} \frac{dk_x}{2\pi/a} \int_{-\pi/a}^{\pi/a} \frac{dk'_x}{2\pi/a} [\tilde{\psi}'^{\dagger}_{+, \sigma}(k_x, k_y), \tilde{\psi}'^{\dagger}_{-, \sigma}(k_x, k_y + Q_y^0)] \\ &\quad \times \begin{pmatrix} \hbar k_x v_F \delta(k_x - k'_x) & \tilde{\Delta}(k_x - k'_x, k_y) \\ \tilde{\Delta}^*(k_x - k'_x, k_y) & -\hbar k_x v_F \delta(k_x - k'_x) \end{pmatrix} \begin{pmatrix} \tilde{\psi}'_{+, \sigma}(k'_x, k_y) \\ \tilde{\psi}'_{-, \sigma}(k'_x, k_y + Q_y^0) \end{pmatrix}, \end{aligned} \quad (2.24)$$

where

$$\tilde{\Delta}(k_x - k'_x, k_y) = \int_{-\infty}^{\infty} dx \bar{\Delta}(x, k_y) \exp[-i(k_x - k'_x)x]. \quad (2.25)$$

The wave function $\tilde{\psi}'_+$ and $\tilde{\psi}'_-$ mix at the Fermi momentum $k_x \approx 0$. The energy gap at the Fermi momentum is given by $|\tilde{\Delta}(0, k_y)|$ and the wave function gets the phase of $\tilde{\Delta}(0, k_y)$ when k_x crosses the Fermi momentum at fixed k_y . Using Eq. (2.5), we find that $\sigma_{xy}/(e^2/h)$ is given by

the winding number of $\tilde{\Delta}(0, k_y)$ around the origin in the complex plane as k_y is changed from $-\pi/b$ to π/b .¹⁸ If we take $\Delta(x) = \Delta_N \exp(iN\delta x)$, we get

$$\begin{aligned} \tilde{\Delta}(0, k_y) &= \Delta_0 I_N(\alpha, \beta) \exp \{ -iNb(k_y - q_y/2) \\ &\quad - i\alpha \sin[2b(k_y - q_y/2)] \\ &\quad + i\beta \cos[b(k_y - q_y/2)] \}. \end{aligned} \quad (2.26)$$

The amplitude of the gap at the Fermi momentum does not depend on k_y and $\tilde{\Delta}(0, k_y)$ turns $(-N)$ times around the origin in the complex plane as k_y is changed from $-\pi/b$ to π/b . Thus the Hall conductance is obtained as $-2Ne^2/h$ as discussed above.

III. MODEL CALCULATION ON SIMPLIFIED STANDARD MODEL

In order to understand why the quantized Hall constant can change its sign as a function of H , we explicitly evaluate $\sigma_{xy}(H)$ by utilizing a simplified standard model, namely, we consider the following mean-field Hamiltonian by rewriting (2.1):

$$\mathcal{H} = \mathcal{H}_0 + \mathcal{H}_1, \quad (3.1)$$

$$\mathcal{H}_0 = - \sum_k (\cos k) C_k^\dagger C_k - v \sum_k (C_k^\dagger C_{k+\delta} + \text{H.c.}), \quad (3.2)$$

$$\mathcal{H}_1 = \sum_n \sum_k \Delta_n C_{k+2k_F+n\delta}^\dagger C_k, \quad (3.3)$$

with the self-consistent equation

$$\mathcal{H} = \int \frac{dk_y}{2\pi} \int dx \Psi^\dagger \begin{pmatrix} iv_F \partial_x - 2v \cos(\delta x - k_y) & \Delta(x) \\ \Delta^*(x) & iv_F \partial_x - 2v \cos(\delta x - k_y) \end{pmatrix} \Psi, \quad (3.5)$$

where the spatial dependence of the OP, $\Delta(x)$, is given by the Fourier transformation in terms of Δ_l as

$$\Delta(x) = \sum_{l=-\infty}^{\infty} \Delta_l e^{il\delta x}, \quad (3.6)$$

$\Psi = [\psi_+(x, k_y), \psi_-(x, k_y)]^T$, and we have explicitly restored the k_y dependence suitable for the present problem. A transformation from Ψ to $\tilde{\Psi}$ through

$$\psi_\pm(x, k_y) = \tilde{\psi}_\pm(x, k_y) \exp[\pm i(2v/v_F \delta) \sin(\delta x - k_y)]$$

yields

$$\mathcal{H} = \int \frac{dk_y}{2\pi} \int dx \tilde{\Psi}^\dagger(x, k_y) \begin{pmatrix} -iv_F \partial_x & \tilde{\Delta}(x, k_y) \\ \tilde{\Delta}^*(x, k_y) & iv_F \partial_x \end{pmatrix} \tilde{\Psi}(x, k_y), \quad (3.7)$$

where

$$\begin{aligned} \tilde{\Delta}(x, k_y) &= \Delta(x) e^{-i\tilde{\alpha} \sin(\delta x - k_y)} \\ &= \sum_{l,n} \Delta_l J_n(\tilde{\alpha}) e^{ilk_y} e^{i(l-n)\delta x}. \end{aligned} \quad (3.8)$$

The scaling parameter $\tilde{\alpha}$ introduced before is given by

$$\tilde{\alpha} = 4v/v_F \delta. \quad (3.9)$$

Instead of varying the magnetic field, which can always

$$\Delta_n = -U \sum_k \langle C_k^\dagger C_{k+2k_F+n\delta} \rangle. \quad (3.4)$$

Here we have dropped the spin index without losing the essence of our problem and introduced $v = t_b/2t_a$ and $t'_b = 0$ ($a = b = 1$). We have assumed $Q_y^0 = 0$. All the energy scales are normalized by t_a . We allow the OP's Δ_n ($n = 0, \pm 1, \pm 2, \dots$) to appear.

The mean-field solution is determined by numerically diagonalizing (3.1)–(3.3) under (3.4) for rational magnetic fields $\phi/\phi_0 = 1/p$. The detailed numerical calculations are given in our previous papers⁷ for the same spinless standard model. The many-order-parameter state can appear irrespective of the filling, δ , v , and U . It has been also shown that the largest OP could be other than Δ_0 , in contrast with what is expected by the Peierls theorem, that the filling uniquely determines the nesting vector of $Q_x = 2k_F$. In this paper we mainly discuss the cases $p = 36$, $u = U/t_a = 1.0$ – 2.0 , and $v = 0$ – 0.2 .

Let us briefly repeat the same argument as in Sec. II with a simplified standard model to set up the formula of the Hall conductance appropriate for our purposes. By linearizing the dispersion relation near the Fermi wave numbers $\pm k_F$, (3.1) can be rewritten in x representation as

be approximated by a fractional form via $H = (\phi_0/ab)(q/p)$, we can effectively change H by varying v through this scaling factor $\tilde{\alpha}$, which determines all the physical quantities. In the following we regard the change of H as the change of v . It is seen that the energy gap at $\pm k_F$ is determined by $2|Z(k_y)|$ where the complex function

$$Z(k_y) = \sum_{l=-\infty}^{\infty} \Delta_l J_l(\tilde{\alpha}) e^{ilk_y} \quad (3.10)$$

has been introduced. Thus our next task is to find a mean-field solution to evaluate (3.10) in order to know its winding number, which gives rise to the Hall constant L .

IV. SINGLE-ORDER-PARAMETER-LIKE STATE

Among various types of FISDW states which satisfy the self-consistency condition (3.4), we first discuss the single-OP-like state where the largest OP distinctly exceeds many other smaller OP's in magnitude. This type of solution is expected to be stable near the FISDW–normal-state boundary. As shown in Fig. 3(a) the FISDW subphases successively change via a first-order transition as a function of v , or $1/H$ through the scaling factor $\tilde{\alpha}$ defined by (3.9). The corresponding Hall numbers are shown in Fig. 3(b), and faithfully reflect the numbering of the largest OP in these subphases. Therefore the situation is virtually same as in the single-OP state because the second or third largest OP's are so small

compared with the largest OP. It is interesting to compare the energy gaps at the Fermi level E_F calculated by two means. (1) Twice the minimum value $2|Z(k_y)|_{\min}$ of the complex $Z(k_y)$ function against $0 < k_y \leq 2\pi$ gives an estimate of the gap at E_F in the linearized dispersion approximation [see Fig. 3(c)]. (2) The direct diagonalization for the mean-field Hamiltonian without linearization gives the whole band structure, thus allowing one to estimate the gap at E_F [see Fig. 3(d)]. Shown in Fig. 4 is an example of the band structure, displaying a distinct gap opened at E_F . Comparing Figs. 3(c) and 3(d) it is seen that both behave similarly, including the magnitudes, implying that the linearization approximation is rather accurate at least for smaller u values. It is also interesting to notice from these figures that toward the phase boundaries the gap at E_F understandably decreases, signaling the instability of that state. The overall band-structure change against v or H^{-1} is shown in Fig. 5(a) and the enlarged band structure near E_F in Fig. 5(b). The former shows that as v increases the band tends to become fragmented from the upper and lower band edges while keeping the maximum energy gap opened at E_F . The numbers in Fig. 5(b) denote the Hall number at that state and the position of E_F below which the states are filled. As v increases, the energy gap at E_F tends to decrease, reflecting the fact that the nesting is deteriorating.

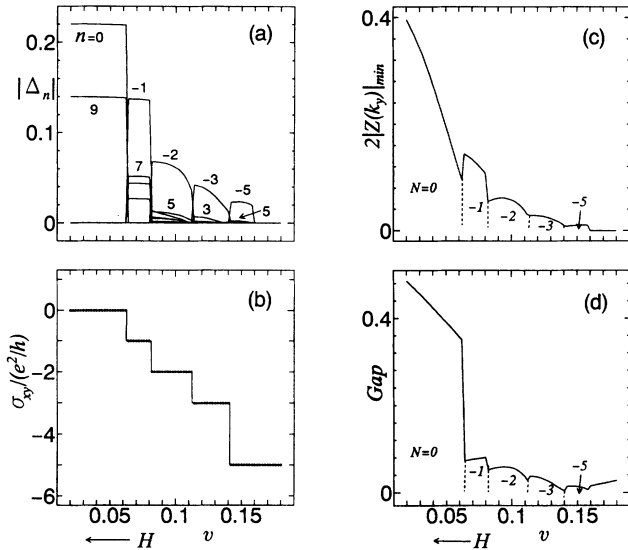


FIG. 3. Single-order-parameter-like solutions of the mean-field equations (3.1)–(3.4), which have a single dominant component of the order parameters, and the corresponding Hall number as a function of v ($u=1.5, \delta/2\pi=\frac{1}{36}$). (a) The magnitudes for various order parameters $|\Delta_n|$ where the subphases change successively via a first-order transition. (b) The corresponding Hall numbers calculated by (2.5), showing that the Hall step corresponds to the subphase transition, and (c) the associated energy-gap closings evaluated by taking the minimum of the energy gap $2|Z(k_y)|$. (d) The energy-gap closings obtained from direct band-structure calculations. The numbers in (c) and (d) denote the numbering of each integer subphase. The energy scale is normalized by t_a .

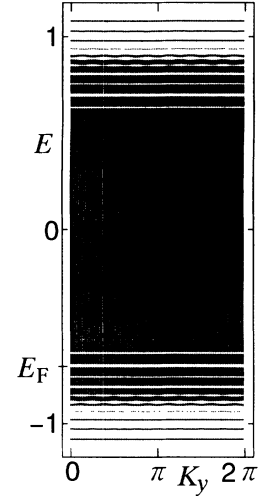


FIG. 4. Band structure as a function of k_y ($0 \leq k_y < 2\pi$; $b=1$) for the mean-field solution displayed in Fig. 3 ($u=1.0$, $v=0.038$, and $\delta=2\pi/36$), in which Δ_0 is largest. The energy scale is normalized by t_a . It is seen that the nine subbands from the bottom among the total 36 bands are occupied, yielding a large gap between the occupied and the unoccupied states above (the band is quarter filled in our case).

Beyond a certain critical value of v the mean-field solution ceases to exist.

V. MULTIPLE-ORDER-PARAMETER STATE AND SIGN AND REVERSAL OF THE HALL CONSTANT

In this section we consider a genuine multiple-order-parameter state where many OP's with comparable magnitudes coexist. This type of solution is expected to be realized in the ground state because the fully fledged OP's are competing. This situation is different from the FISDW-normal-state boundary where a distinctive OP dominates, stabilizing the single-OP-like state mentioned in the previous section.

As shown in Fig. 6, several MOP states are found as a mean-field solution for the given parameters of the problem, all satisfying a local minimum condition. These MOP states have almost equal energies. The number in each figure denotes the Hall number calculated by counting the winding number of $Z(k_y)$ defined in (3.10). It is seen that the Hall number does not necessarily correspond to the numbering of the largest OP for a given MOP state. According to (3.10) the winding number is determined by summing up all contributions from the MOP's where the MOP's are interfering with each other.

We display in Fig. 7(a) the v dependence or H dependence of a MOP state in which the OP's change little, but continuously evolve. Since the energy gap at E_F or the Hall constant determined by $Z(k_y)$ does depend on v and $\tilde{\alpha}$ through the Bessel function $J_l(\tilde{\alpha})$ as seen from (3.10), the Hall constant can vary even in such a case and exhibits a sign reversal as shown in Fig. 7(b). When the Hall number exhibits a jump, the energy gap at E_F must be closed there. It is seen from Fig. 7(c) that the energy gap at E_F evaluated by finding a minimum of $2|Z(k_y)|$ tends

to diminish toward the Hall steps. As ν varies, $Z(k_y)$ must cross the origin in the complex plane in order to change the winding number if the MOP state continuously evolves as shown in Fig. 8, where the Hall number changes from $+1$ to -2 in this case, corresponding to the Hall step in Fig. 7(c).

It is now obvious that since the Hall constant is determined by a delicate combination of MOP's $\{\Delta_N\}$, the Hall jump occurs even when two MOP states with similar sequences of MOP's transform within a single integer subphase domain via a first-order transition. This situation is illustrated in Fig. 9 where the two MOP states with the same largest (Δ_0) and second largest (Δ_9) OP's interchange as a function of ν at which the energies of the two solutions are crossed. The corresponding Hall num-

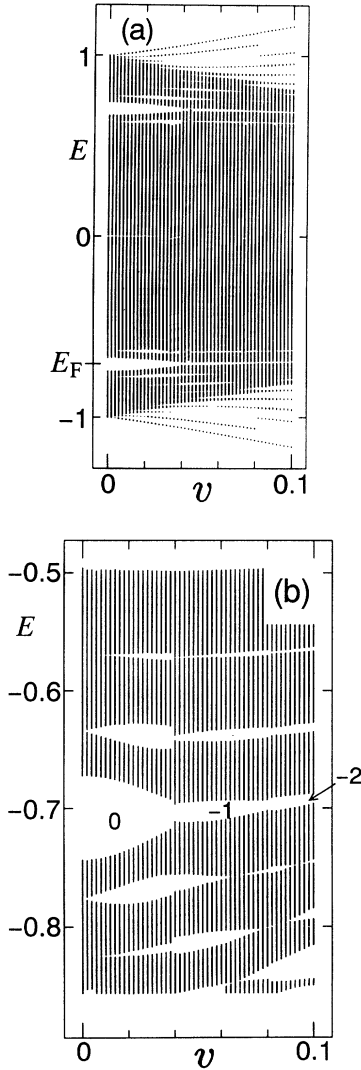


FIG. 5. Energy bands normalized by $2t_a$ as a function of ν , corresponding to Fig. 3 ($u=1.5$ and $\delta/2\pi=\frac{1}{36}$). (a) Global band structure and (b) band structure near the Fermi level E_F where the numbers denote the corresponding Hall constant and the position of E_F . It is seen that the energy gap decreases when the subphase boundary is approached. Also compare Figs. 3(c) and 3(d).

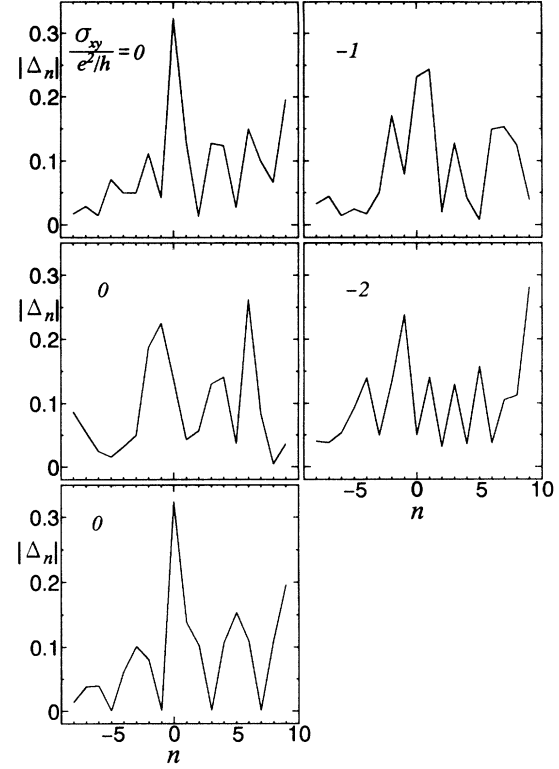


FIG. 6. Various mean-field solutions under fixed parameters ($u=2.0, \nu=0.1$, and $\delta/2\pi=1/36$) and the corresponding Hall constant. Each panel shows the distribution of the order parameters $|\Delta_n|$ for each solution and the Hall constant. The energy is normalized by t_a . It is seen that, depending on the detailed combination of various OP's, the Hall constants are widely different from solution to solution. The energies of these solutions are almost degenerate.

ber exhibits a jump at that point, in addition to the other type of jumps due to the reason mentioned above, as shown in Fig. 9(b).

VI. CONCLUSIONS AND DISCUSSIONS

After setting up a general formula for the Hall conductance of a FISDW state, we have explicitly evaluated it for several types of mean-field solutions for a simplified standard model and found in general that the numbering N of the integer subphases ($N=0,1,2,3,\dots$) does not necessarily correspond to the Hall number L given by $\sigma_{xy}=2Le^2/h$ because the FISDW is characterized by a set of multiple order parameters $\{\Delta_n\}$ ($n=0,\pm1,\pm2,\pm3,\dots$) whose largest OP is Δ_N . It should be noted in passing that the quantized Hall conductance $\sigma_{xy}/(e^2/h)=2L$ for the FISDW is always an even integer because L is an integer. This must be checked experimentally.

We have provided an explanation why the quantized Hall constant changes its sign in the FISDW problem and explicitly demonstrated that the sign reversal of the Hall conductance can occur as a function of H in terms of the concept of the multiple-order-parameter state. A necessary condition for the sign reversal to occur is that a

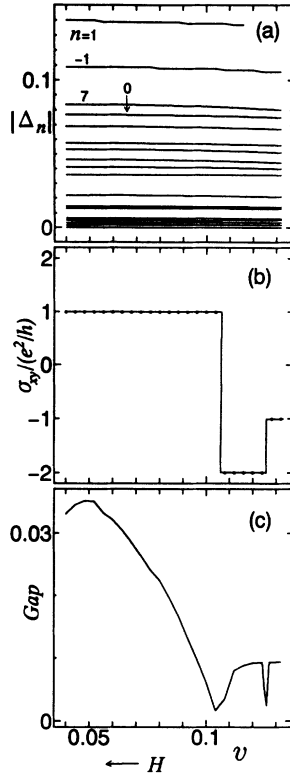


FIG. 7. Mean-field solution of (3.1)–(3.4) with multiple order parameters and sign reversal of the Hall constant as a function of ν ($u = 1.5, \delta/2\pi = \frac{1}{36}$). (a) The magnitudes for various order parameters Δ_n . (b) The corresponding Hall numbers calculated by (2.5), and (c) the associated energy-gap closings evaluated by taking the minimum of the energy gap $2|Z(k_y)|$.

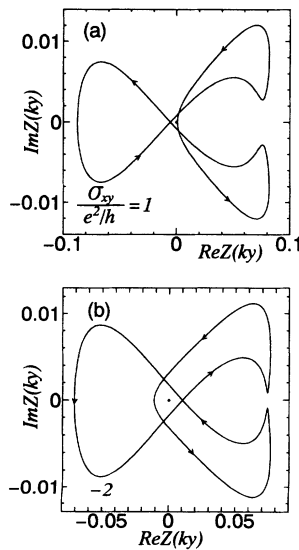


FIG. 8. Change of the winding number of the complex function $Z(k_y)$ from 1 to -2 [$\text{Im}Z(k_y)$ vs $\text{Re}Z(k_y)$], corresponding to Fig. 7 where around $\nu \approx 0.1$ the sign reversal of the Hall constant ($1 \rightarrow -2$) occurs.

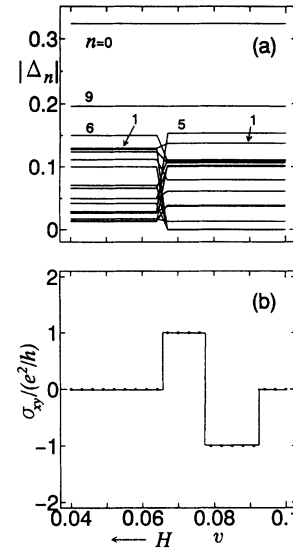


FIG. 9. Example of the first-order phase transition as a function of ν or $1/H$ where the largest and the next largest OP keep their order intact ($u = 2.0$ and $\delta/2\pi = 1/36$). (a) The third largest OP and others are changed at the first-order transition. (b) The Hall conductance exhibits a jump at the transition point in addition to the jumps when the state is continuously evolving.

FISDW subphase contains multiple order parameters $\{\Delta_n\}$ with both signs of $n=0, \pm 1, \pm 2, \pm 3, \dots$. This concept also enables us to understand the cascade phenomenon of successive phase transitions. This feature is absent in the naive standard theory^{3–5} of the single-order-parameter state. In the case where a FISDW state continuously evolves against H , the jumps of the Hall constant must be accompanied by a gap closing. We have points out another possibility of the sign reversal, associated with the first-order phase transition where the underlying FISDW subphases with different Hall number simply transform. This can occur even within one integer subphase domain in which the largest order parameter does not alter. This might be the case in $X = \text{PF}_6$, where

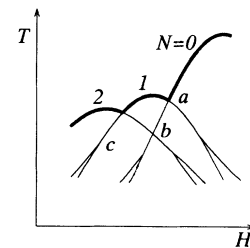


FIG. 10. Possible phase diagram of H vs T (schematic). Thin (thick) lines indicate a first- (second-) order phase transition. Two second- and two first-order lines meet at a point, giving rise to a tetracritical point denoted by a . Two first-order lines intersect each other denoted by b . Branching out of a first-order line into two first-order lines gives rise to a tricritical point denoted by c . These three kinds of phase transitions are collectively called the cascade phenomenon.

the sign change of the Hall conductance is observed^{8,13} within a subphase either $N=2$ or $N=3$, as shown in Fig. 1.

So far we only consider the magnetic field of the form $\phi/\phi_0=1/p$. In this case, all k_x points whose number is p are connected to each other through t_b . When the field is given by a form $\phi/\phi_0=q/p$ where p and q ($\neq 1$) are mutually prime, $\delta=(q/p)(2\pi/a)$ is a multiple of q in p -divided k_x reciprocal space. A "fractional" order parameter of the form $\Delta_{n+m/q}$ with $m=1,2,\dots,q-1$, whose wave number is $Q_x=2k_F+(n+m/q)\delta$, becomes possibly nonvanishing. Indeed, as shown before,⁷ the fractional OP's are finite in a mean-field solution in general. While the fractional OP plays an important role in forming the density wave, it plays a negligible role for the Hall conductance because we can always reassign the fractional OP $\Delta_{n+m/q}$ to some "integer" OP $\Delta_{n'}$, where n' is at least of order p , which is a large number. Therefore, the contribution from such an OP with large integer index is negligible in view of (3.10), as $J_p(\tilde{\alpha})$ is practically zero even when $\Delta_{n+m/q}$ is nonvanishing. It is also noted that the OP's with smaller index contribute to σ_{xy} more effectively than those with larger ones because of the same $J_n(\tilde{\alpha})$ factor.

We sketch a possible phase diagram of H vs T in Fig. 10, where the thick (thin) line indicates a second- (first-) order phase transition and each "cell" surrounded by transition lines is characterized by a particular set of MOP's, each corresponding to a subphase. On the FISDW-normal-state boundary two second-order and two first-order transition lines meet at a point, constituting a tetracritical point. This has been observed experimentally.¹⁷ At lower T there are at least two possibilities for the topology of the phase transition lines: (1) intersection of two first-order lines and (2) branching out of one first-order line into two. Both types are observed experimentally^{9,17} as cascade phenomena. The corresponding Hall-constant behavior $\sigma_{xy}(H)$ when sweeping H under a fixed T is difficult to predict from the present calculation, since except for the integer subphase just beneath the normal-state boundary in which the largest OP is $N=0,1,2,\dots$ from high field, the lower sub-subphases, sub-sub-subphases and sub-sub-sub-subphases, etc., are difficult fully characterize, with subtle and slight differences. Basically the numbering N of the integer subphase indicated in Fig. 10 roughly corresponds to the Hall number $L=2N$, giving rise to a Hall step. However, in particular near the integer subphase boundary where various OP's are comparable in magnitude, the Hall number L can differ from that numbering and could be positive or negative. It is highly desirable to establish the H vs T phase diagram at lower T (which is lacking presently) and to perform detailed Hall-constant measurements in order to check whether or not the Hall step always corresponds to some phase transition.

In connection with the $X=\text{ClO}_4$ problem,¹ it is noted that the phase diagram in H vs T is quite distorted, contrary to that expected from the standard theory, because of the presence of the anion ordering at 24 K. The sign reversal in this particular case might be explained in a more conventional way. If we slightly extend the stan-

dard model, the ordering of the integer subphases can be made different from $N=0,1,2,3,\dots$, giving rise to the sign reversal of the Hall conductance. That is, getting back to the original standard model, the transition to FISDW is realized for those values of N and Q_y^0 , which give the maximum of $|I_N(\alpha,\beta)|^2$ defined by (2.22), as shown by Virosztek, Chen, and Maki.⁴ They have shown that the maximum of $|I_N(\alpha,\beta)|^2$ is realized for $N=\dots,-4,-3,-2,-1,0$ in this order as H is increased. The transitions between the subphases with different N are first order. In the parameter regions around $\eta=2t_b/t'_b=50$ the FISDW's with $N>0$ are not realized. However, if we take a smaller value of η , which is possible in the case of large next-nearest-neighbor hoppings in the b direction, N does not change monotonically. We can show that the sequence of the subphase numbering for $\eta=2$ is $N=\dots,-2,-1,+1,0$, and thus the sign reversal might occur.

We also show another example that the sign of Hall conductance is changed by increasing the magnetic field. We extend the standard model as

$$\epsilon_{\perp}(k_y) = -2t_b \cos(bk_y) - 2t'_b \cos(2bk_y - \theta) - 2t_3 \cos(3bk_y), \quad (6.1)$$

where the parameter θ gives a $\sin(2bk_y)$ term, which has been introduced by Yamaji⁶ and the third-neighbor hopping t_3 is also introduced. Then $I_n(\alpha,\beta)$ in (2.22) is replaced by

$$I_n(\alpha,\beta,\delta,\theta) = i^n \sum_{l,m} (-1)^m e^{il\theta} J_l(\alpha) \times J_{n-2l-3m}(\beta) J_m(\gamma), \quad (6.2)$$

where $\gamma=2t_3 \sin(3bq_y/2)/(3t'_b \tilde{H})$. If $\theta=\pi/2$ and $\gamma=0$, we can show that $\max|I_N|^2 = \max|I_{-N}|^2$, i.e., the phases with N and $-N$ are degenerate. Therefore, it is not surprising that sign of the Hall conductance is changed from $2Ne^2/h$ to $-2Ne^2/h$ for $\theta \approx \pi/2$ and $\gamma \approx 0$, in which FISDW of N and $-N$ are almost degenerate. If the transition temperature of even N is suppressed by anion ordering as recently shown by Osada, Kagoshima, and Miura,²⁴ the successive transitions such as $N=\dots,-5,+3,-3,-1$ may be possible for suitably chosen parameters.

Finally, we would like to emphasize the significance of the present problem. As mentioned in Sec. I, the two-dimensional electron system on a lattice under a perpendicular magnetic field is nothing but the so-called Hofstadter problem²¹ widely discussed in various contexts. The resulting recursive band structure as a function of H (the butterfly diagram) is very intriguing and contains deep physics. The calculated Hall conductance²⁰ associated with prominent gaps is indeed quantized and differs widely from gap to gap, including sign changes. The estimated required magnetic field strength (a few megagauss) for the natural unit cell (a few Å by a few Å) is far beyond present-day technology. However, by introducing the electron interaction and inducing density-wave formation, the enlarged supercell now effectively reduces the required magnetic-field strength to a moderate value

(a few tesla) as discussed in Sec. II. The density-wave (charge or spin) state always keeps the Fermi level pinned inside the energy gap in order to stabilize the condensate, which is a necessary condition to observe quantized Hall plateaus; thus we do not need localized electronic state as in the quantized Hall conductance in a two-dimensional

electron liquid at the interface of two semiconductors under a perpendicular field. The two mysteries discussed in this paper, the recursive phase diagram in H vs T or cascade phase transitions and the sign reversal of the quantized Hall conductance, are deeply related to each other and also to the Hofstadter problem.

-
- ¹See, for a review, P. M. Chaikin, W. Kang, S. Hannahs, and R. C. Yu, *Physica B* **177**, 353 (1992).
- ²L. P. Gor'kov and A. G. Lebed, *J. Phys. (Paris) Lett.* **45**, 433 (1984).
- ³K. Yamaji, *J. Phys. Soc. Jpn.* **54**, 1034 (1985).
- ⁴K. Maki, *Phys. Rev. B* **33**, 4826 (1986); A. Virosztek, L. Chen, and K. Maki, *ibid.* **34**, 3371 (1986); L. Chen and K. Maki, *ibid.* **35**, 8462 (1987).
- ⁵G. Montambaux, M. Héritier, and P. Lederer, *Phys. Rev. Lett.* **55**, 2078 (1985).
- ⁶K. Yamaji, *J. Phys. Soc. Jpn.* **56**, 1841 (1987).
- ⁷K. Machida, Y. Hori, and M. Nakano, *Phys. Rev. Lett.* **70**, 61 (1993); Y. Hori, K. Kishigi, and K. Machida, *J. Phys. Soc. Jpn.* **62**, 3598 (1993). Also see K. Machida and M. Nakano, *ibid.* **59**, 4223 (1990); K. Machida, Y. Hori, and M. Nakano, *ibid.* **60**, 1730 (1991); Y. Hori and K. Machida, *ibid.* **61**, 1246 (1992).
- ⁸J. R. Cooper, W. Kang, P. Auban, G. Montambaux, D. Jérôme, and K. Bechgaard, *Phys. Rev. Lett.* **63**, 1984 (1989); L. Brossard, B. Piveteau, D. Jérôme, A. Moradpour, and M. Ribault, *Physica B* **143**, 406 (1986).
- ⁹G. Faini, F. Pesty, and P. Garoche, *J. Phys. (Paris) Colloq.* **49**, C8-807 (1988); F. Pesty, P. Garoche, and M. Héritier, in *The Physics and Chemistry of Organic Conductors*, edited by G. Saito and S. Kagoshima, Springer Proceedings in Physics Vol. 51 (Springer, Berlin, 1990), p. 87; F. Pesty and P. Garoche, *Fizika (Zagreb)* **21**, Suppl. 3, 40 (1989); F. Tsobnang, F. Pesty, P. Garoche, and M. Héritier, *Synth. Met.* **42**, 1707 (1991); F. Tsobnang, F. Pesty, P. Garoche, and M. Héritier, *J. Appl. Phys.* **73**, 5651 (1993). Also see U. Scheven, W. Kang, and P. M. Chaikin, *J. Phys. (Paris) Colloq.* **3**, C2-287 (1993).
- ¹⁰M. Ribault, *Mol. Cryst. Liq. Cryst.* **119**, 91 (1985).
- ¹¹W. Kang, S. T. Hannahs, and P. M. Chaikin, *Phys. Rev. Lett.* **70**, 3091 (1993).
- ¹²S. T. Hannahs, J. S. Brooks, W. Kang, L. Y. Chiang, and P. M. Chaikin, *Phys. Rev. Lett.* **63**, 1988 (1989).
- ¹³P. M. Chaikin (private communication).
- ¹⁴W. Kang, J. R. Cooper, and D. Jérôme, *Phys. Rev. B* **43**, 11 467 (1991).
- ¹⁵D. Poilblanc, G. Montambaux, M. Héritier, and P. Lederer, *Phys. Rev. Lett.* **58**, 270 (1987); also see M. Kohmoto, *J. Phys. Soc. Jpn.* **59**, 1537 (1990).
- ¹⁶P. Středa, *J. Phys. C* **15**, L1299 (1982).
- ¹⁷F. Tsobnang, F. Pesty, and P. Garoche (unpublished).
- ¹⁸V. M. Yakovenko, *Phys. Rev. B* **43**, 11 353 (1991).
- ¹⁹D. J. Thouless, M. Kohmoto, M. P. Nightingale, and M. den Nijs, *Phys. Rev. Lett.* **49**, 405 (1982).
- ²⁰Y. Hasegawa, Y. Hatsugai, M. Kohmoto, and G. Montambaux, *Phys. Rev. B* **41**, 9174 (1990).
- ²¹D. R. Hofstadter, *Phys. Rev. B* **14**, 2239 (1976).
- ²²Preliminary work, Y. Hasegawa, K. Machida, M. Kohmoto, and V. M. Yakovenko (unpublished).
- ²³M. Kohmoto, *Phys. Rev. B* **39**, 11 943 (1989).
- ²⁴T. Osada, S. Kagoshima, and N. Miura, *Phys. Rev. Lett.* **69**, 1117 (1992).

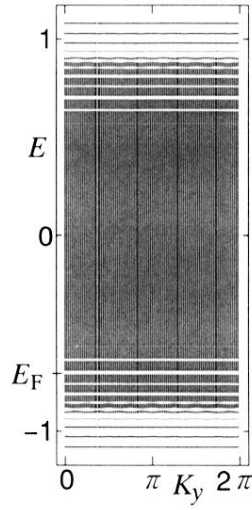


FIG. 4. Band structure as a function of k_y ($0 \leq k_y < 2\pi$; $b=1$) for the mean-field solution displayed in Fig. 3 ($u=1.0$, $v=0.038$, and $\delta=2\pi/36$), in which Δ_0 is largest. The energy scale is normalized by t_a . It is seen that the nine subbands from the bottom among the total 36 bands are occupied, yielding a large gap between the occupied and the unoccupied states above (the band is quarter filled in our case).